Further Probing the Mechanisms Driving Projected Subtropical Decreases of Extreme Precipitation Intensity.

Thabo Msawenkosi Agrippa Mpanza (thbms17@gmail.com)
York University - Keele Campus: York University https://orcid.org/0000-0002-6622-3771
Neil Tandon
York University - Keele Campus: York University

Research Article

Keywords: extreme precipitation, atmospheric dynamics, climate change, future projections, cloud-resolving model, climate model

Posted Date: May 6th, 2021

DOI: https://doi.org/10.21203/rs.3.rs-462492/v1

Abstract

Regional projections of extreme precipitation intensity (EPI) are strongly influenced by regional projections of “extreme ascent,” i.e. ascending air during periods of extreme precipitation. Earlier studies have performed analysis suggesting that long-term changes in eddy length scale and vertical stability are key factors influencing extreme ascent projections, but these mechanisms have yet to be confirmed with controlled model experiments. In this study, we perform such controlled experiments using a cloud-resolving model (CRM). The selected CRM domains are two locations over the subtropical South Atlantic Ocean where global climate models consistently project weakening of extreme ascent with accordingly decreased EPI. At each study location, three pairs of 20-year maximum precipitation events are simulated with the CRM, with each pair consisting of an event during the historical period (1981-2000) and an event during the future period (2081-2100), with large-scale forcings for the three pairs derived from three different members of an initial condition ensemble of the Canadian Earth System Model version 2 (CanESM2). These experiments reveal that, in both study locations, weakening of differential cyclonic vorticity advection (dCVA) is a key driver of projected decreases in extreme ascent and EPI. Weakening of dCVA is expected in accordance with hydrostatic balance because, as temperatures warm, the pressure spacing between geopotential surfaces increases. Although there is evidence that the CRM is more sensitive to dCVA changes than CanESM2, such a dCVA mechanism may nonetheless be important to consider for EPI changes in the real world.

Full Text

This preprint is available for download as a PDF.

Figures

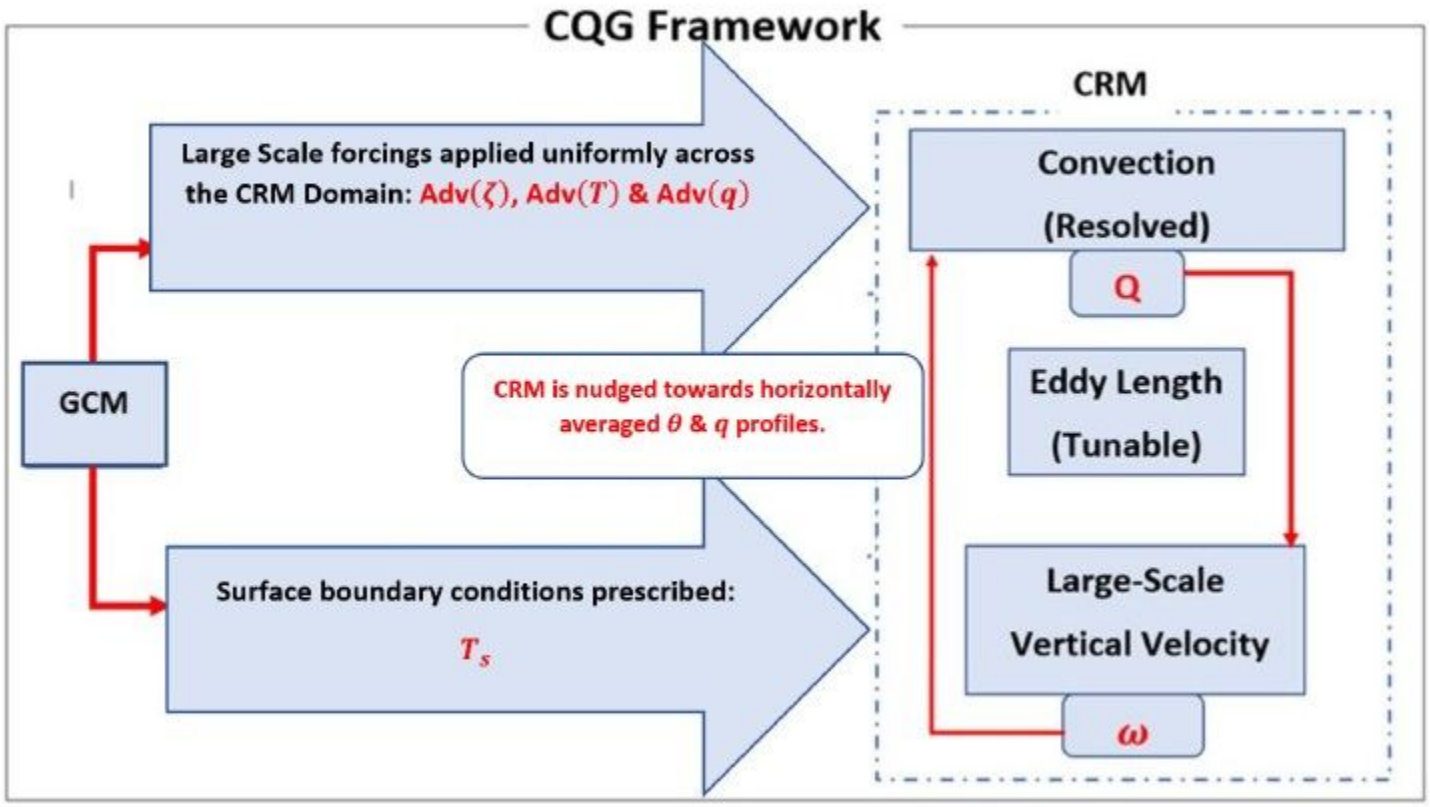

Figure 1

Schematic diagram of the column quasigeostrophic (CQG) framework used in this study.

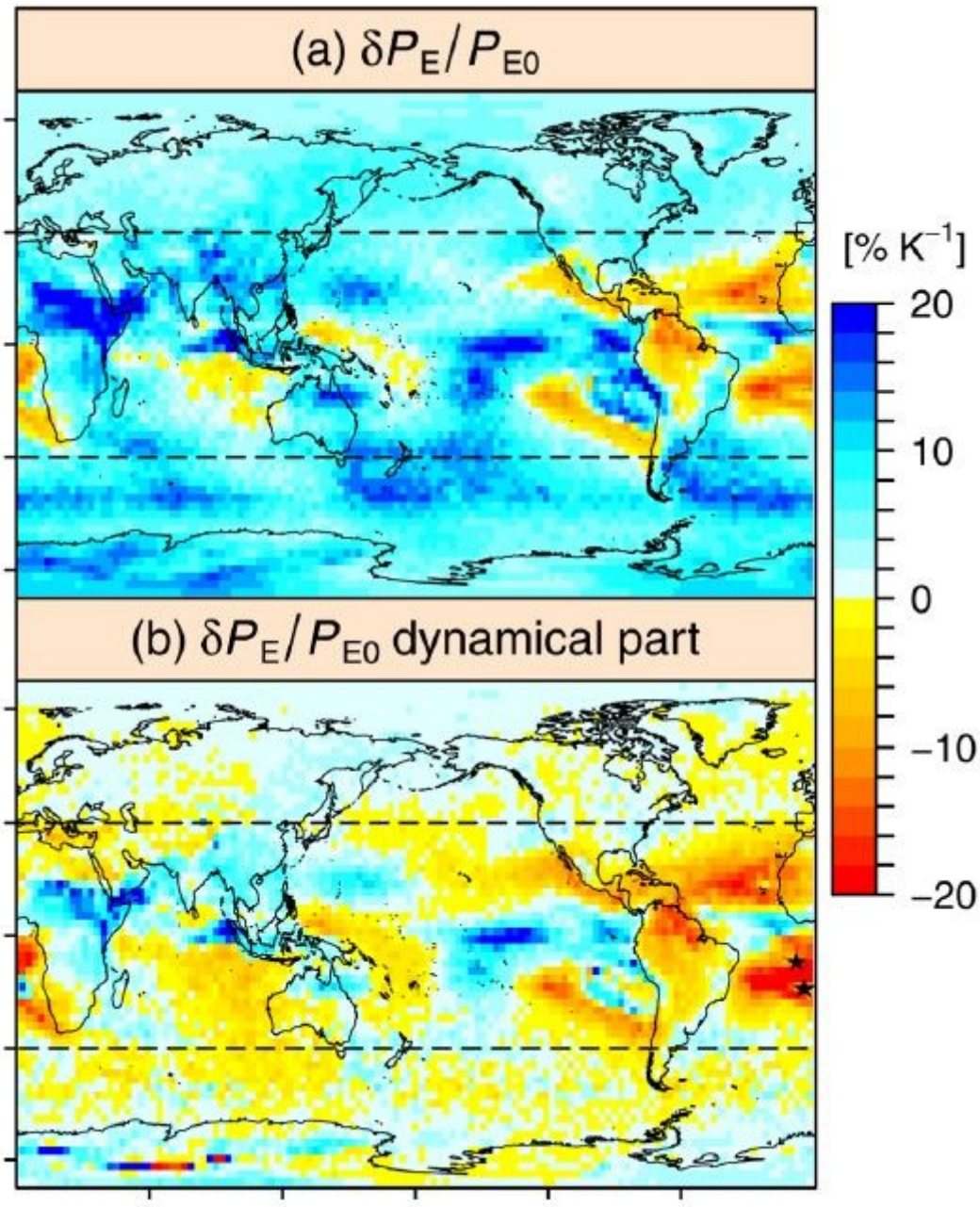

Figure 2

(a) Composite climatic change in 10-year maximum of daily precipitation and (b) its dynamical part normalized by zonal mean climatic change in surface temperature, computed from the CanESM2 large ensemble (adapted from Tandon et al, 2018b). See Tandon et al (2018b) for details of these calculations. The stars indicate the locations used for the dynamical downscaling experiments in the current study. The black star corresponds to the “S27” study location, and the green star corresponds to the “S18” study location. Note: The designations employed and the presentation of the material on this map do not imply the expression of any opinion whatsoever on the part of Research Square concerning the legal status of any country, territory, city or area or of its authorities, or concerning the delimitation of its frontiers or boundaries. This map has been provided by the authors.

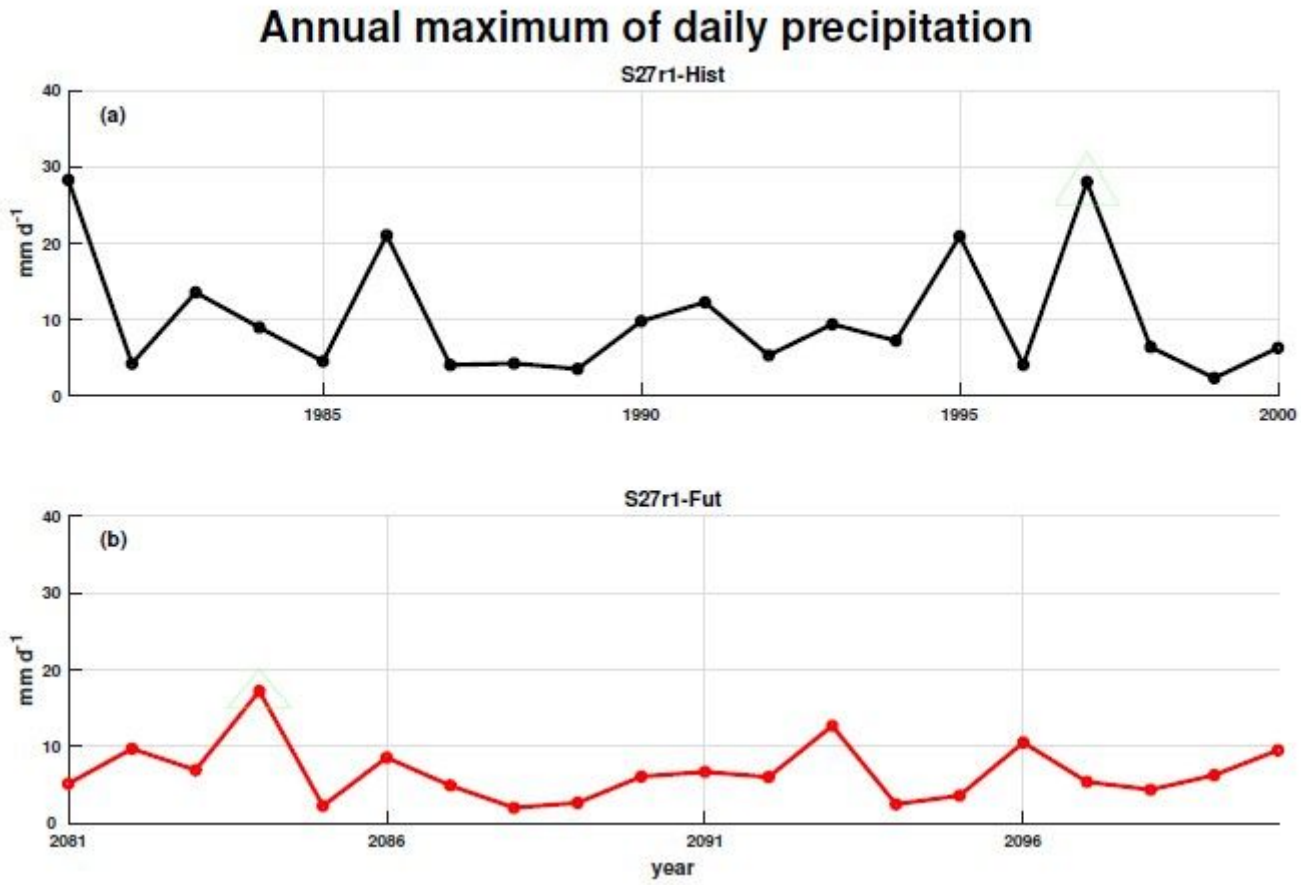

Figure 3

Timeseries of annual maximum daily precipitation over the S27 study location in CanESM2 ensemble group 1 ensemble member 4 during the (a) historical period (1981-2000) and (b) future period (2081-2100). The green triangles indicate the 20-year maximum events chosen for our CRM experiments. See the text for additional details.

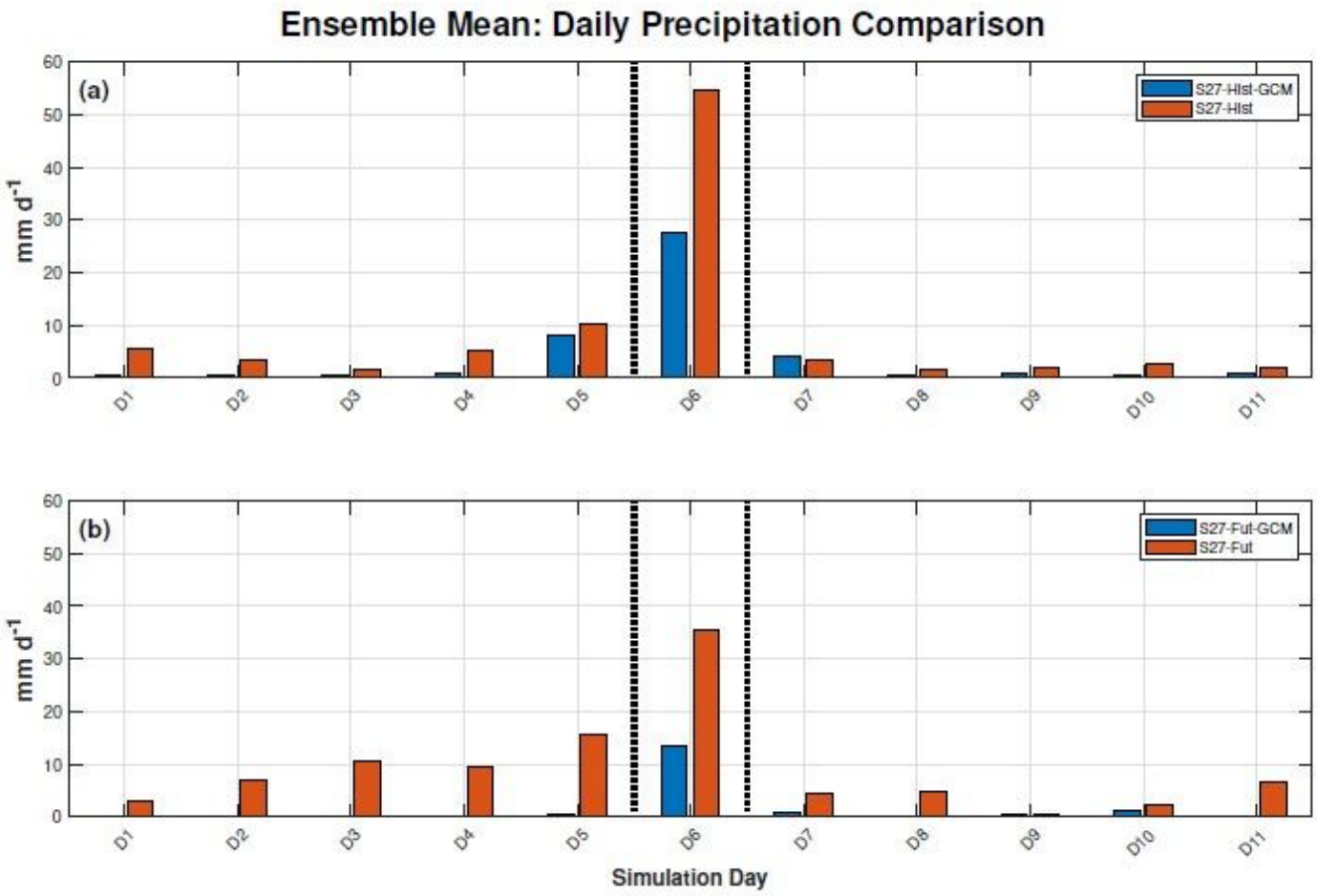

Figure 4

Ensemble mean comparison of the CanESM2 (blue) and CRM (red) daily precipitation timeseries for the 11-day periods centered around the 20-year maxima of extreme precipitation (“simulation day 6,” between the vertical dotted lines) over the S27 region during the (a) historical period and (b) future period. In this and subsequent figures, some CRM timeseries have been time shifted by 1-2 days prior to ensemble averaging so that the day of maximum precipitation aligns with that in the GCM runs. Additional details are provided in Table 3 and the text.

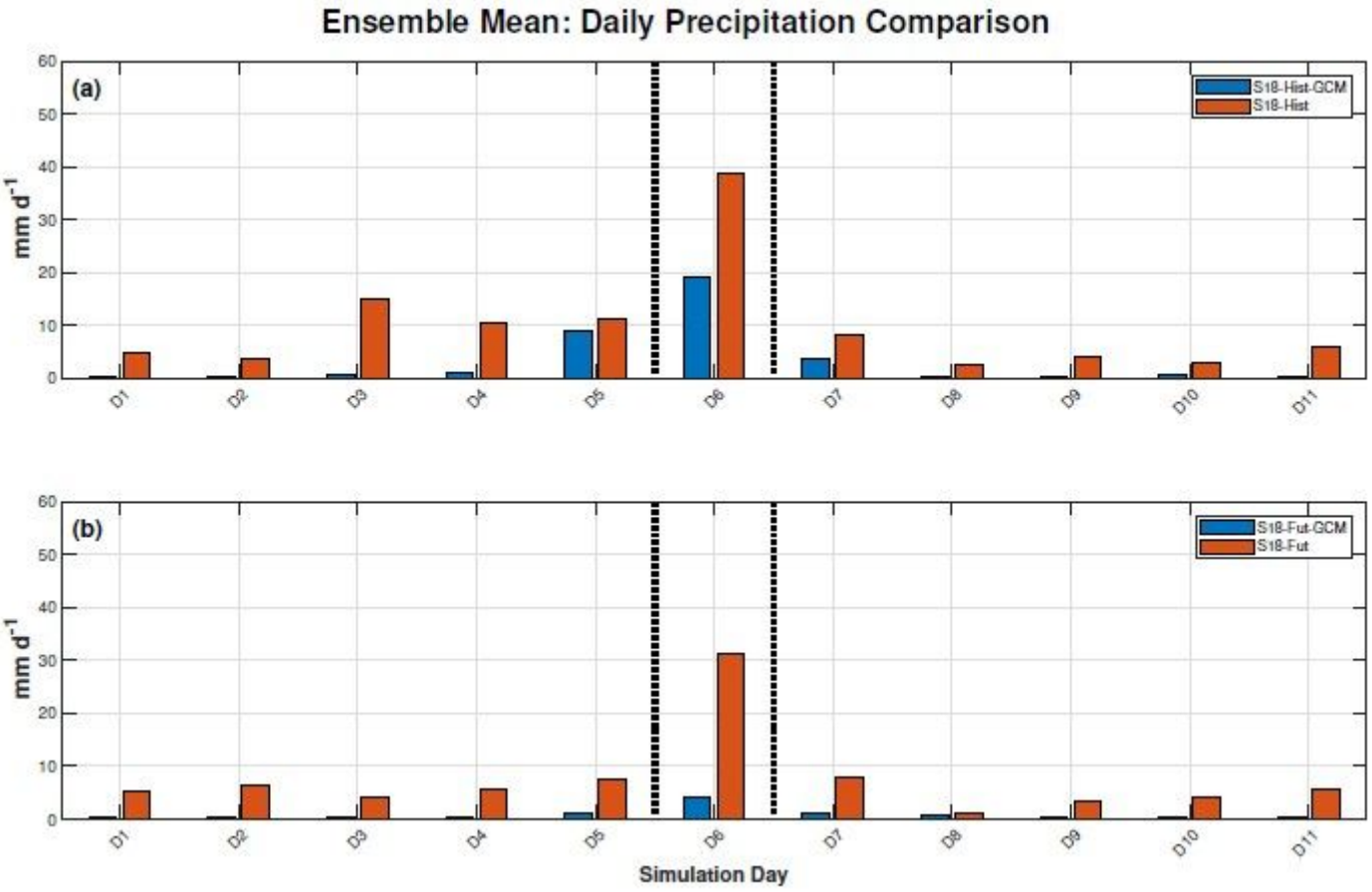

Figure 5

As in Fig. 4 for the S18 study location.

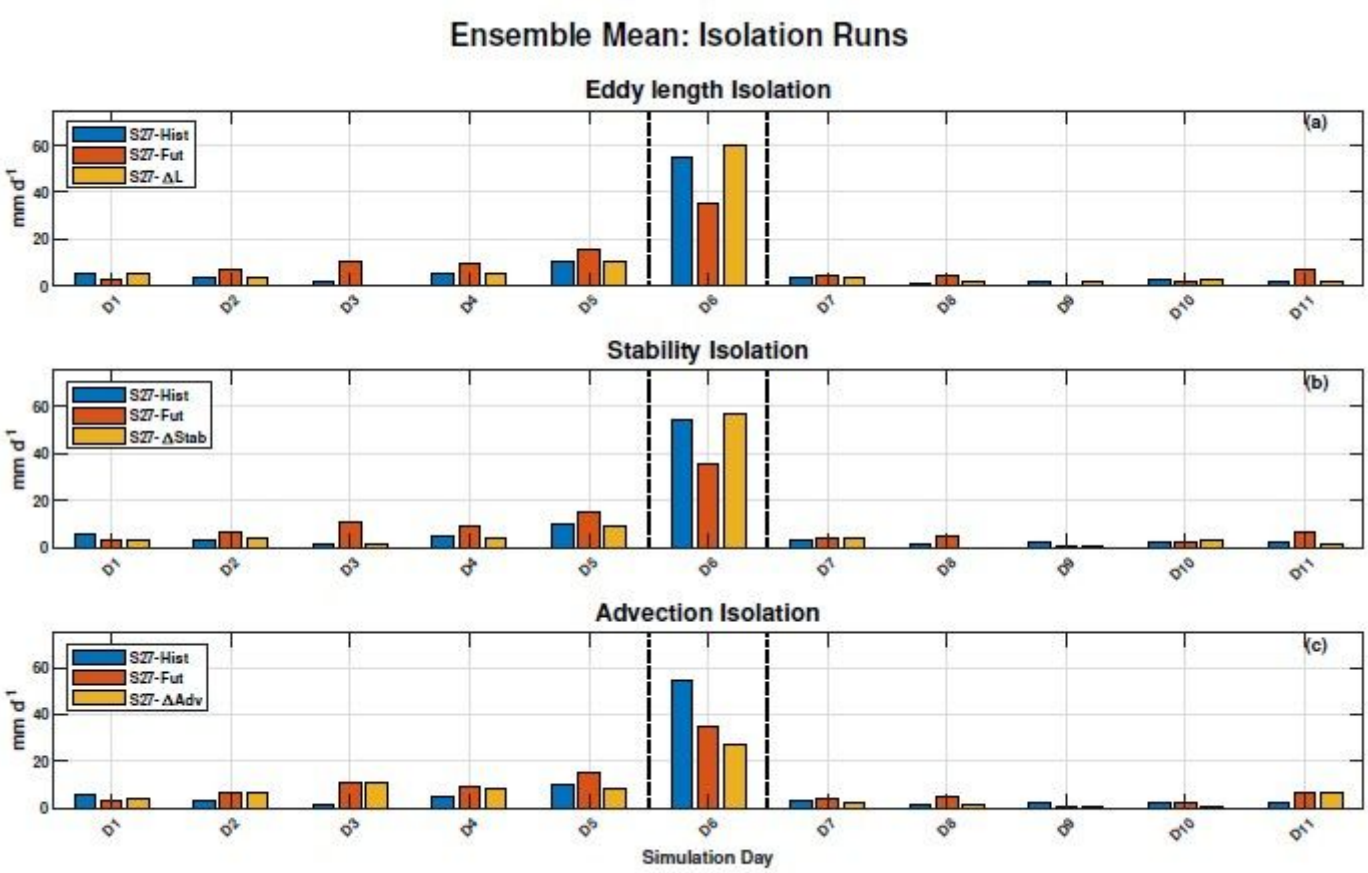

Figure 6

Comparison of ensemble mean daily precipitation timeseries for various CRM isolation runs over the S27 location. (a) S27-Hist (blue), S27-Fut (red) and S27-ΔL, isolating the eddy length effect (yellow). (b) S27-Hist (blue), S27-Fut (red) and S27-ΔStab, isolating the effects of surface temperature and vertical stability (yellow). (c) S27-Hist (blue), S27-Fut (red) and S27-ΔAdv, isolating the effect of horizontal advection (yellow). The day of extreme precipitation in CanESM2 (day 6) lies between the vertical dotted lines.

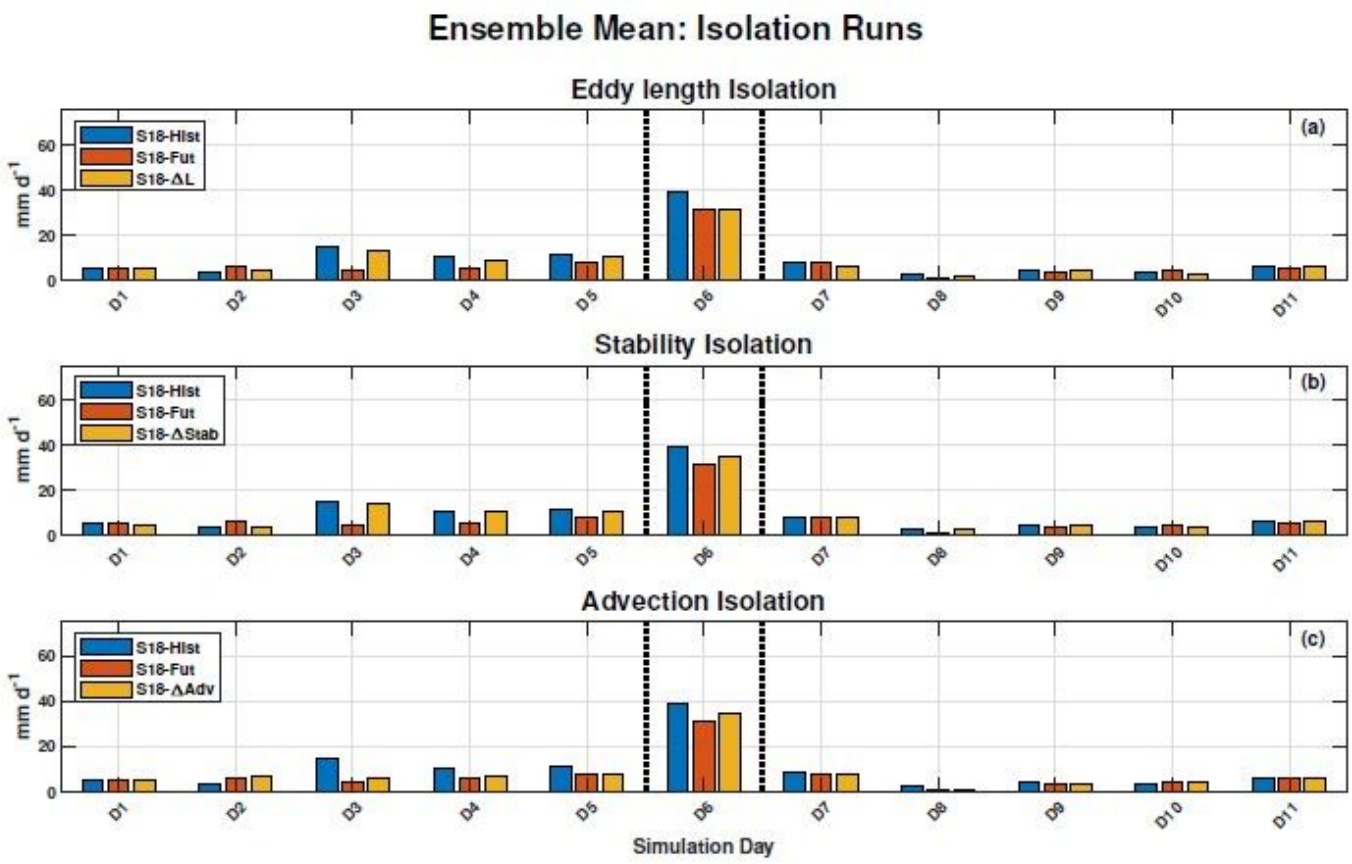

Figure 7

As in Fig. 6 but over the S18 study location.

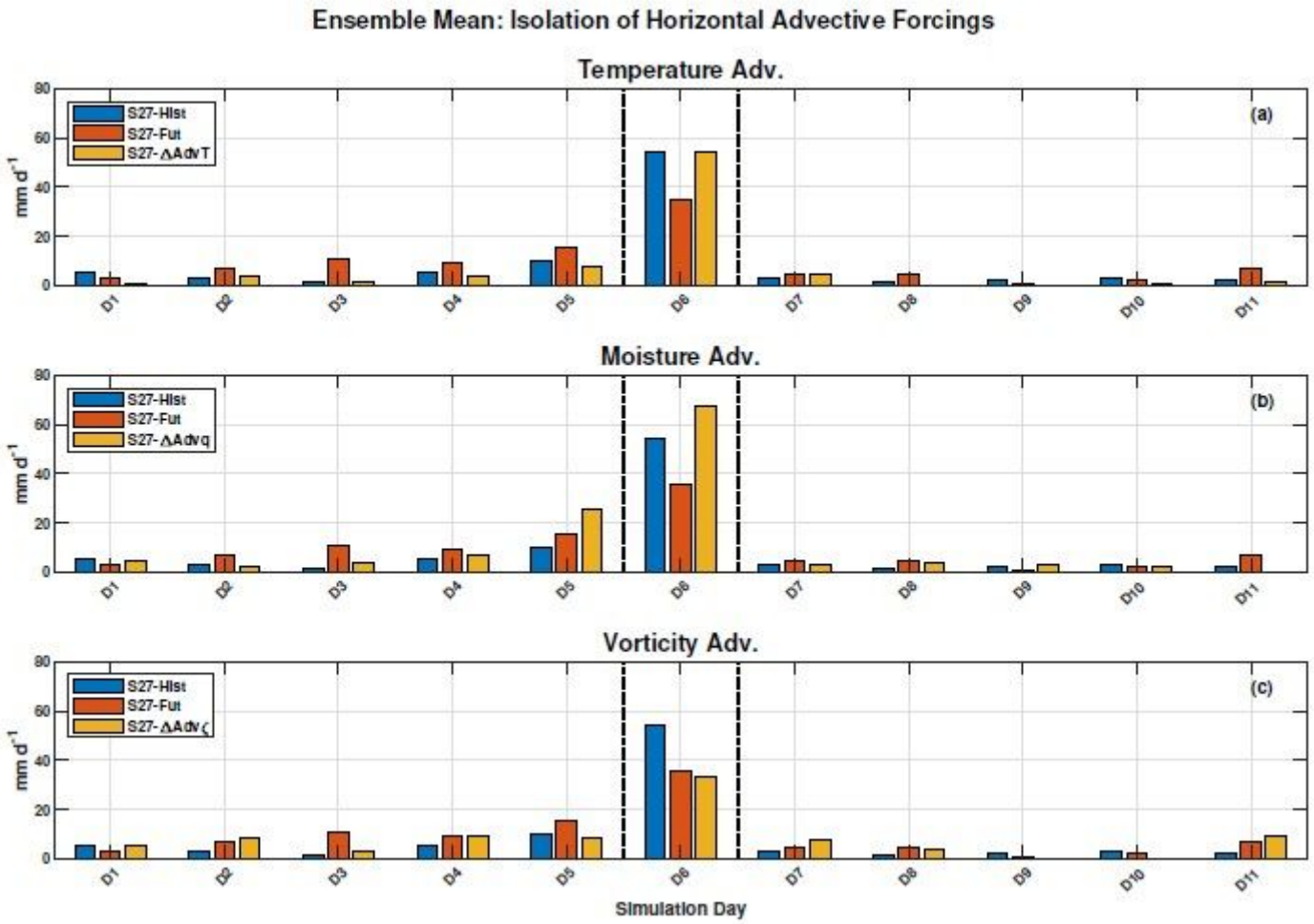

Figure 8

Comparison of daily precipitation timeseries for CRM experiments isolating individual horizontal advective forcings over the S27 location. (a) S27-Hist (blue), S27-Fut (red) and S27-ΔAdvT, isolating the temperature advection effect (yellow). (b) S27-Hist (blue), S27-Fut (red) and S27-ΔAdvq, isolating the moisture advection effect (yellow). (c) S27-Hist (blue), S27-Fut (red) and S27-ΔAdvζ, isolating the vorticity advection effect (yellow). The day of the extreme precipitation in the GCM (“simulation day 6”) lies between the vertical dotted lines.

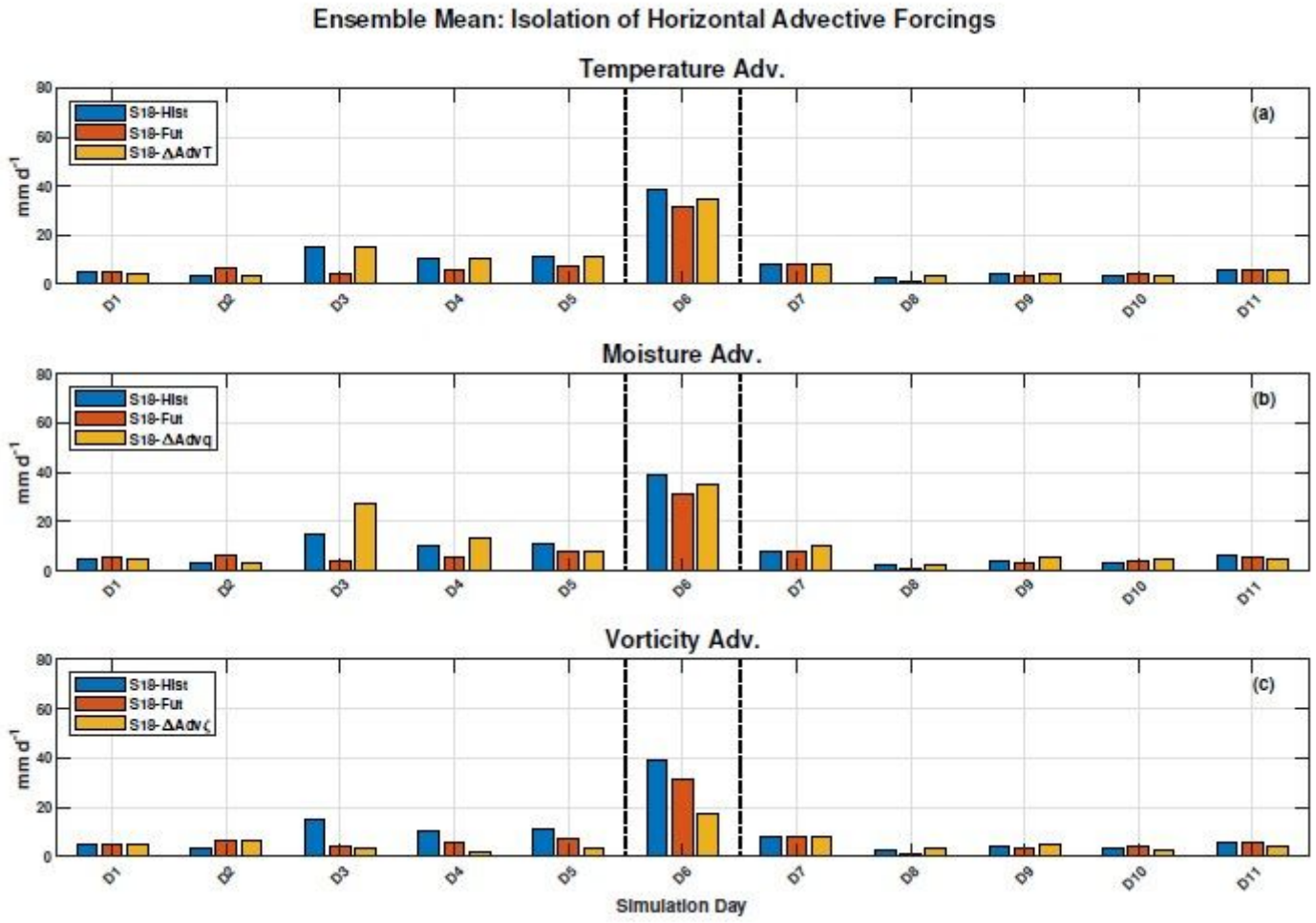

Figure 9

As in Fig. 8 for the S18 study location.

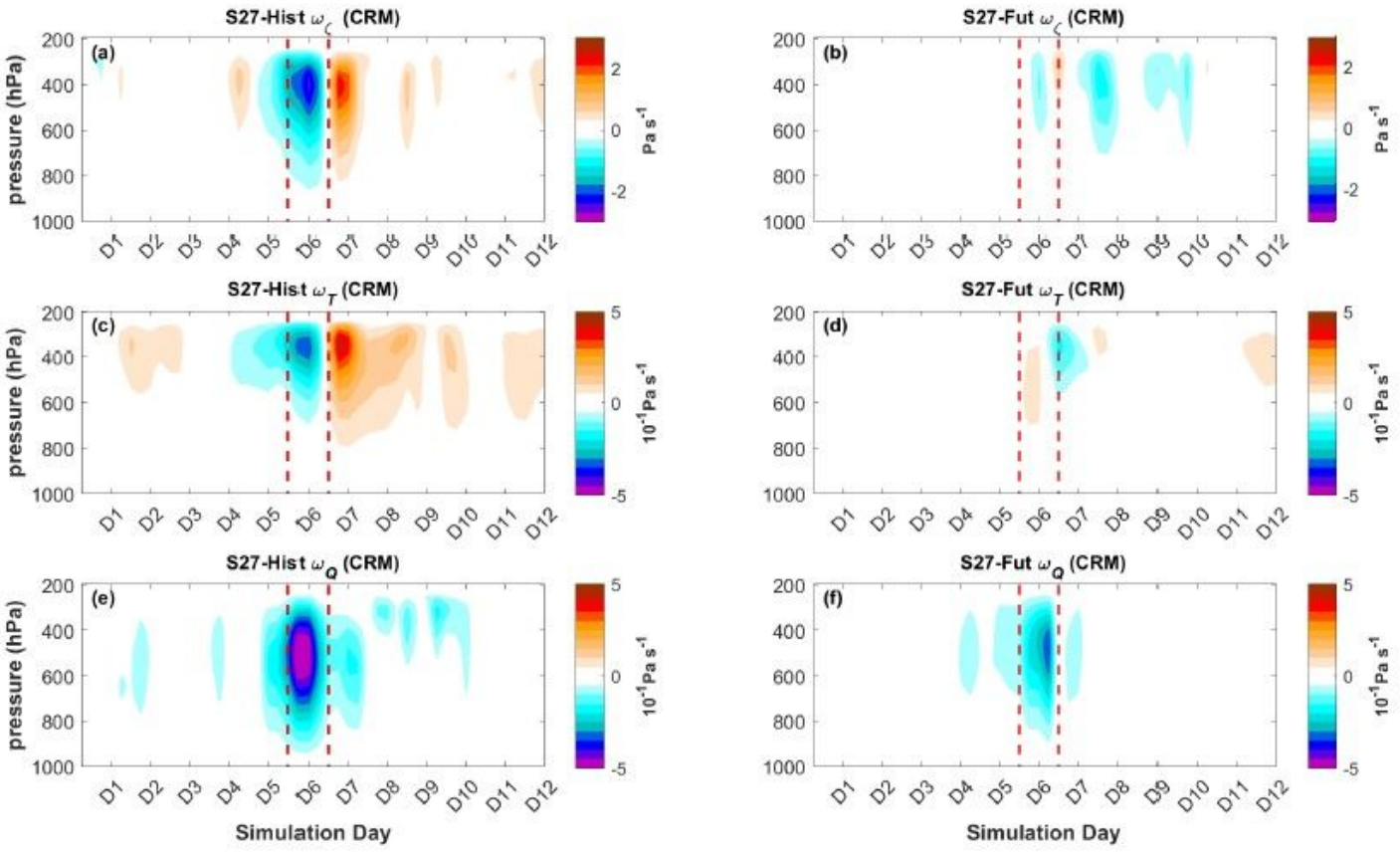

Figure 10

Vertical pressure velocity associated with (a,b) vorticity advection, ωζ, (c,d) temperature advection, ωT, and (e,f) diabatic heating, ωQ, for the (a,c,e) S27-Hist experiments and (b,d,f) S27-Fut experiments. Red dashed lines in each panel mark the beginning and end of the day of extreme precipitation. For clarity, ωT and ωQ are plotted on a scale that is a factor of ten smaller than for ωζ.

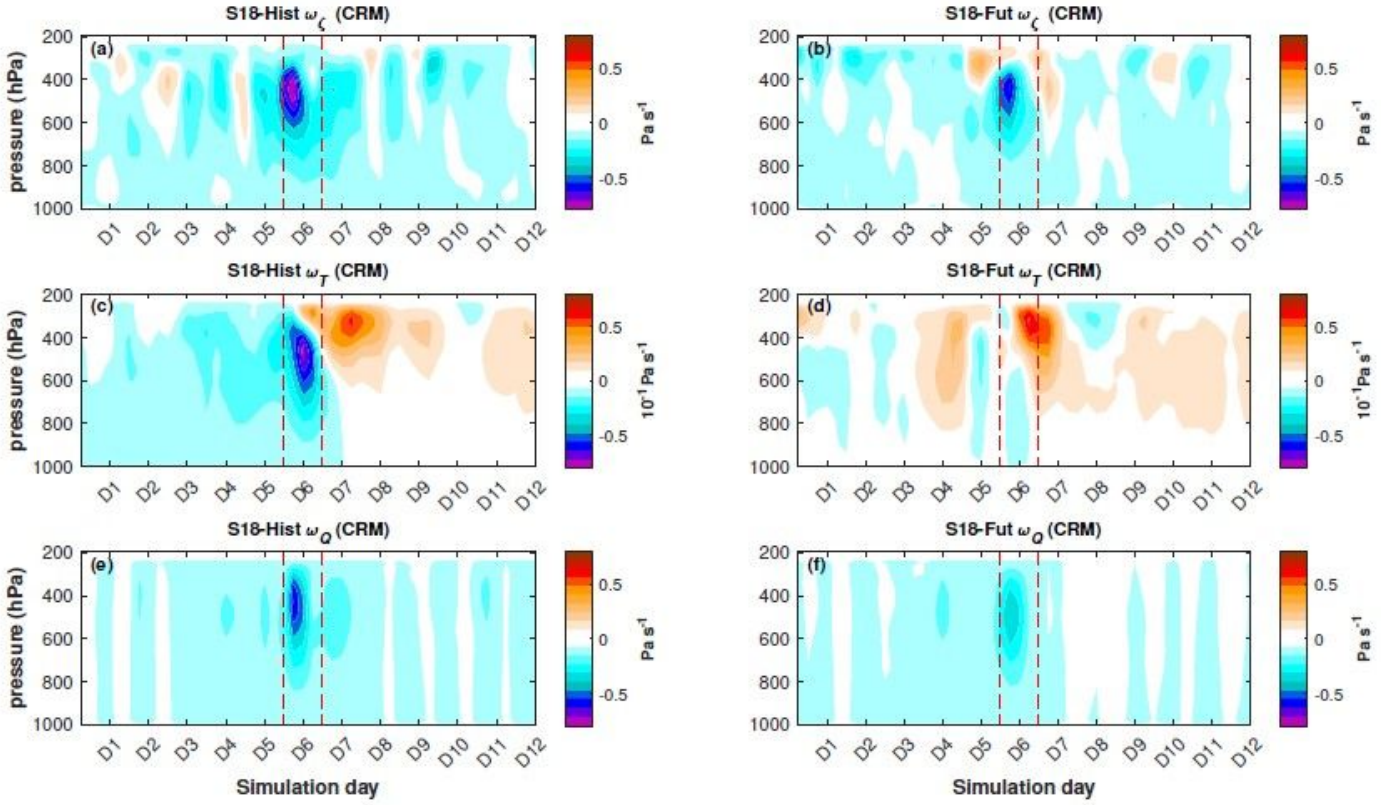

Figure 11

As in Fig. 10 but for the S18 study location. For clarity, panels c and d are plotted on a different scale from the other panels. The scales are different from those used in Fig. 10.

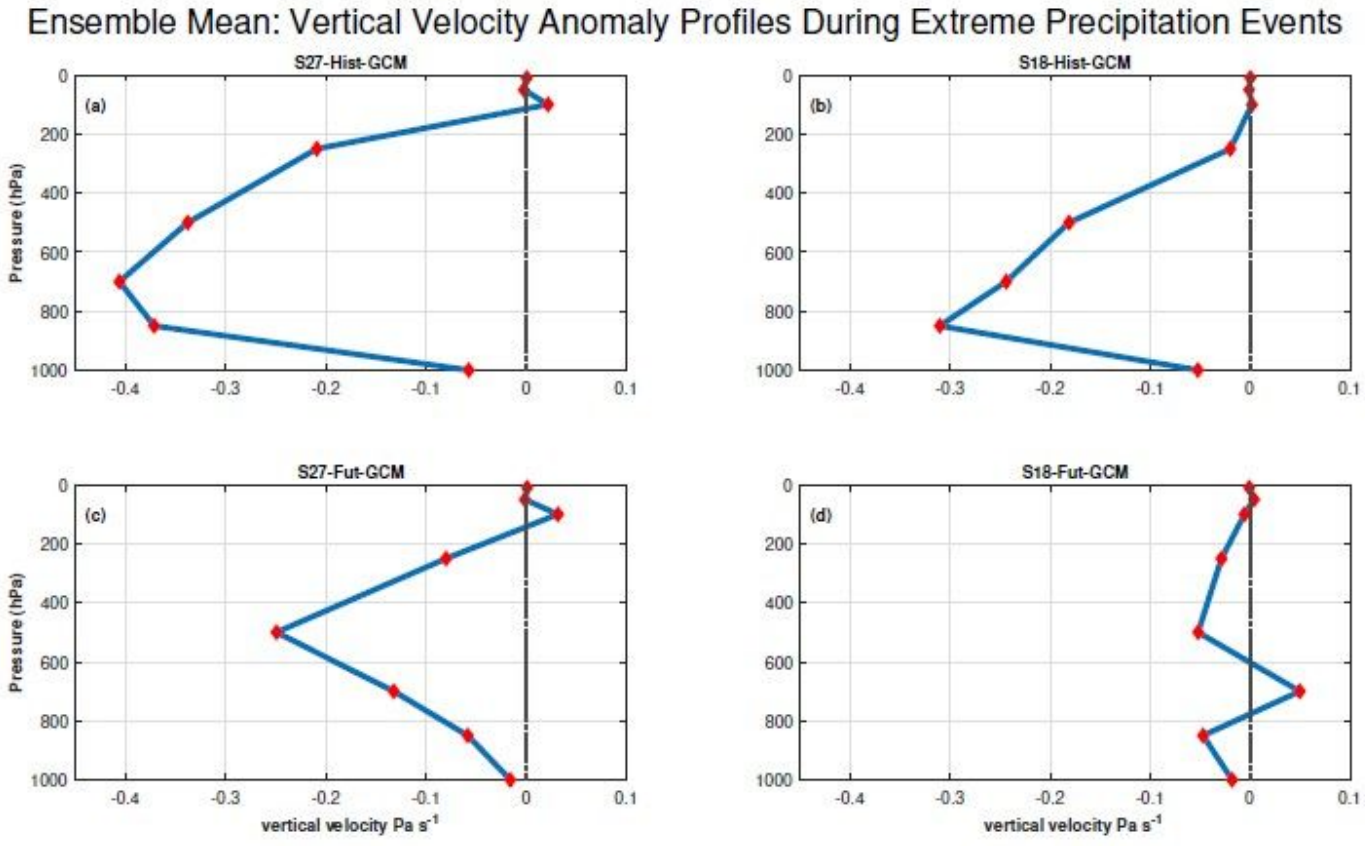

Figure 12

Daily mean vertical pressure velocity profiles on the day of extreme precipitation in the (a) S27- Hist-GCM, (b) S18-Hist-GCM, (c) S27-Fut-GCM and (d) S27-Fut-GCM cases. These profiles have been averaged over the same ensemble members used for the CRM experiments.

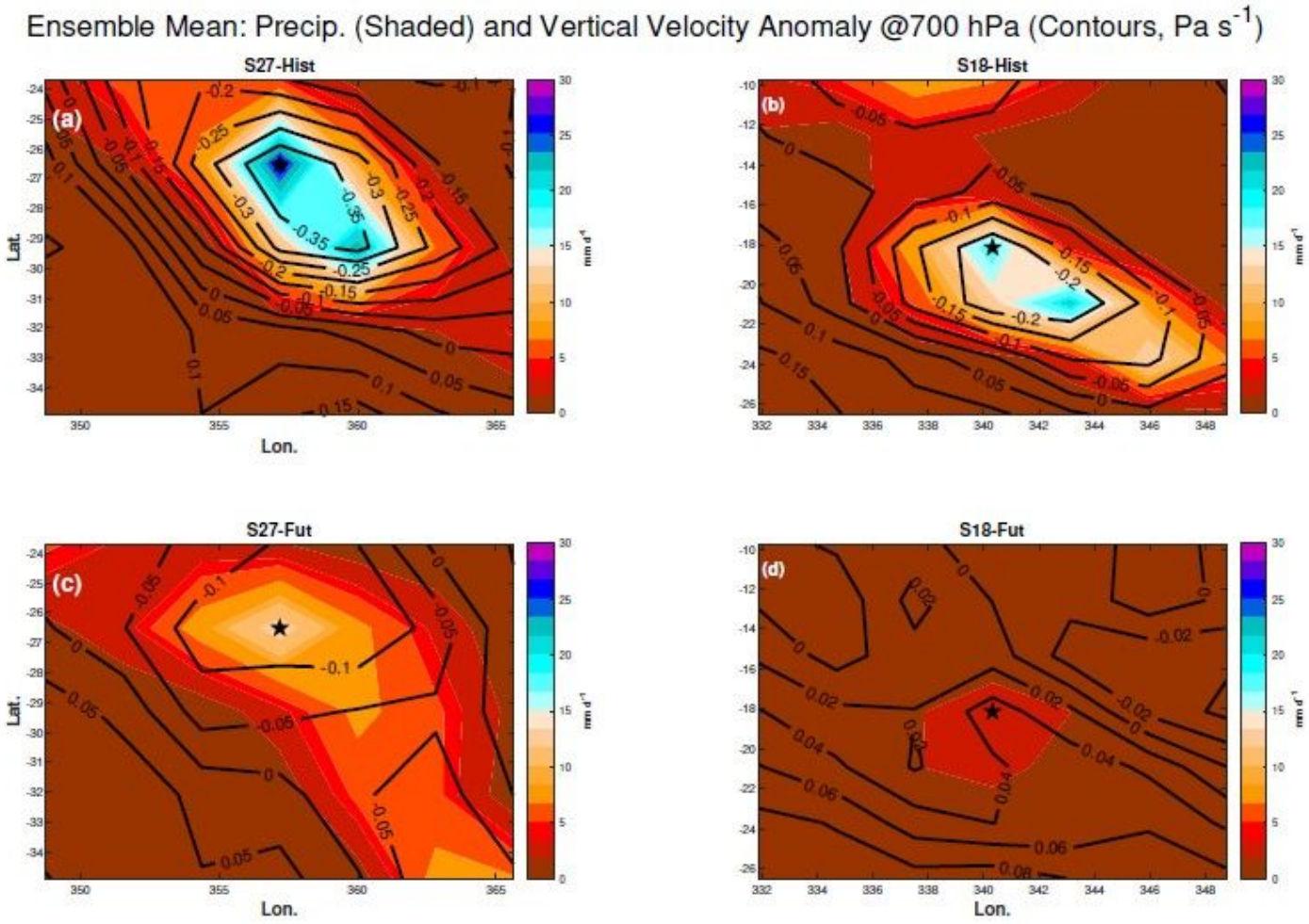

Figure 13

CanESM2 precipitation (shading) and ω at 700 hPa (contours) during EPEs over the (a,c) S27 and (b,d) S18 study locations during the (a,b) historical and (c,d) future periods. The stars indicate the study locations. The fields have been averaged over the same ensemble members used for the CRM experiments.